

Supplementary Information

Highly efficient hydrogen evolution from edge-oriented $\text{WS}_{2(1-x)}\text{Se}_{2x}$ particles on three-dimensional porous NiSe_2 foam

Haiqing Zhou, Fang Yu, Jingying Sun, Hangtian Zhu, Ishwar Kumar Mishra, Shuo Chen, and Zhifeng Ren**

* Correspondence and requests for materials should be addressed to S. C. schen34@uh.edu or Z. F. R. zren@uh.edu.

1. Material and Methods

The ammonium tetrathiotungstate ($(\text{NH}_4)_2\text{WS}_4$, 336734-5g) and selenium (Se, 99.5%, 209651-250g) powders were purchased from Sigma Aldrich. Thermal selenization of commercial Ni foams and the growth of $\text{WS}_{2(1-x)}\text{Se}_{2x}$ particles were carried out in a tube furnace. Before thermal selenization, commercial Ni foam was divided into regular pieces with an estimated geometric area of 1 cm^2 . Then a piece of the 1 cm^2 Ni foam was placed at the center of the furnace and thermally selenized at around 600 °C for 1h with the Se powder supplied at the upstream. For the growth of $\text{WS}_{2(1-x)}\text{Se}_{2x}$ particles, the as-prepared NiSe_2 foams were dipped into a precursor containing $(\text{NH}_4)_2\text{WS}_4$ in dimethylformamide (DMF) solvent (5 wt% in DMF), which were then vacuum dried at 100 °C for 30 min. To grow pure WS_2 or ternary $\text{WS}_{2(1-x)}\text{Se}_{2x}$ particles, we performed thermolysis or a second selenization in a tube furnace at 500 °C with the presence of Ar gas, respectively. After that, the furnace was automatically turned off and cooled down under Ar gas.

The electrochemical performance was studied by an electrochemical station (Gamry, Reference 600). The hybrid catalysts, a Pt wire and a saturated calomel electrode (SCE) were served as the working, counter and reference electrodes, respectively. All the tests were performed under saturated N₂ atmosphere (Matheson, 99.9999%). We have calibrated the reference electrode by a Pt wire in H₂ gas (Matheson, 99.9999%). All the potentials reported here were calibrated to a RHE with a value of 0.263 V difference. The cycling tests were conducted to investigate the catalyst stability at a scan rate of 50 mV/s and potential ranges from 0.06 V to - 0.2 V. Linear sweep voltammetry was utilized to gather the polarization curves at a scan rate of 2 mV/s. All the curves were reported with iR compensation. Chronoamperometry was also carried out to study the time-dependent current density at a specific potential of - 0.145 V. Cyclic voltammetry (CV) curves were collected at different scan rates in the potentials from 0.1 V to 0.2 V, so as to evaluate the double-layer capacitance values. Finally, the electrochemical impedance spectroscopy (EIS) spectra were gathered at a constant potential of - 0.15 V, and the frequencies varied from 10 mHz to 1 MHz. A simplified Randles circuit was applied to fit the EIS spectra.

2. The morphologies of the starting Ni foam and as-prepared NiSe₂ foam

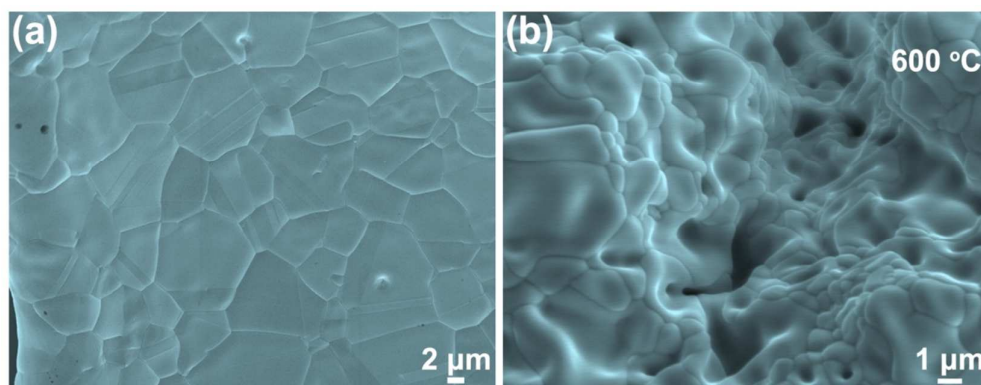


Figure S1. High-magnification SEM images of the starting Ni foam (a) and as-prepared porous NiSe₂

foam grown at 600 °C (b). It is clear that the starting Ni foam is composed of many Ni grains in the Ni region. Instead, there are more porous structures in the NiSe₂ region after selenization.

3. Characterization of as-prepared NiSe₂ samples by XRD and XPS

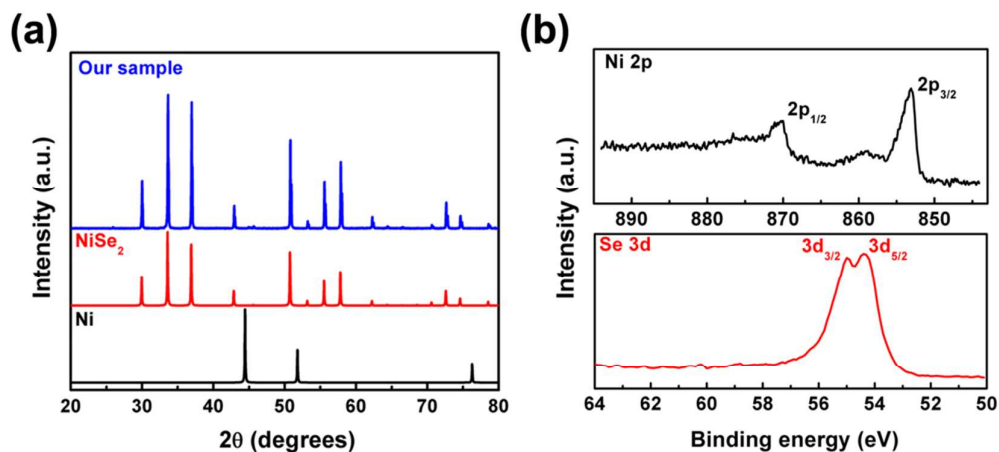


Figure S2. Characterization of the as-prepared NiSe₂ foams by powder X-ray diffraction (XRD) (a) and XPS (b). It is evident that the main compound is pyrite NiSe₂, rather than other nickel selenides, and very small fraction of metallic Ni exists in the as-prepared samples.

4. Typical XPS spectrum of Ni 2p region on WS_{2(1-x)}Se_{2x}/NiSe₂ hybrid catalyst

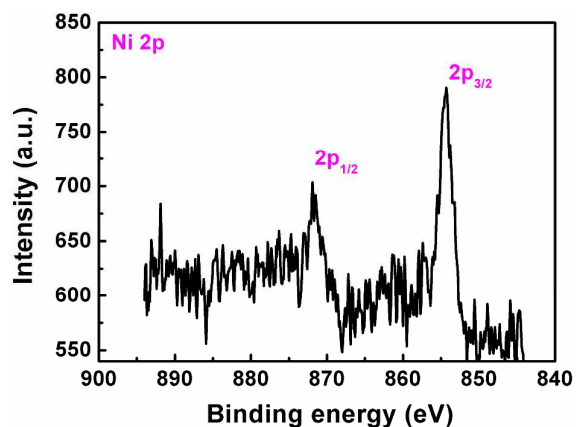


Figure S3. XPS spectrum of Ni 2p region collected on WS_{2(1-x)}Se_{2x}/NiSe₂ hybrid catalyst.

5. Energy dispersive X-ray spectrum (EDS) of the tungsten compound

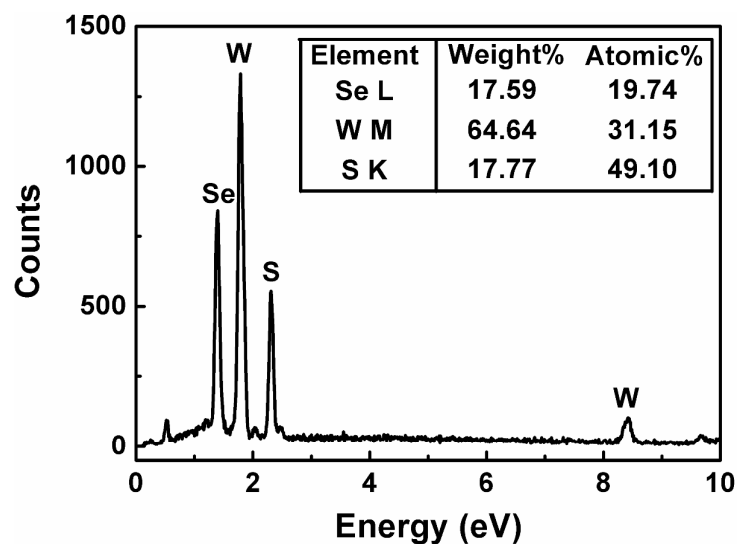


Figure S4. EDS analysis on the chemical composition of as-prepared $WS_{2(1-x)}Se_{2x}$ particles aggregating and extruding from the edge of $NiSe_2$ region.

6. Capacitance measurements

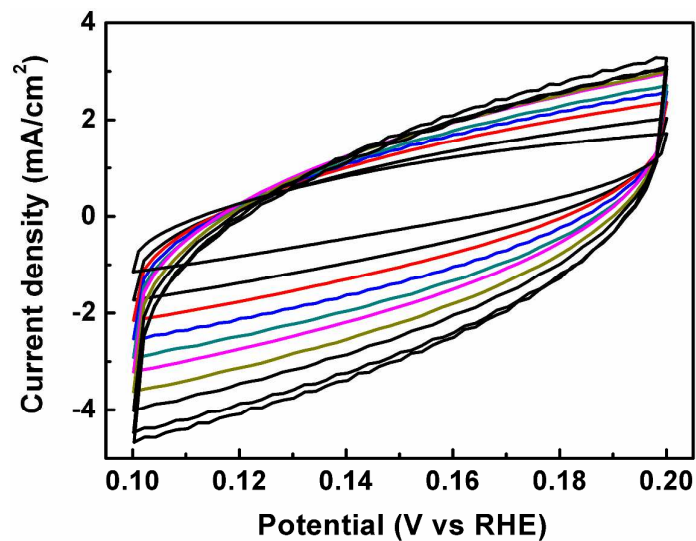


Figure S5. Electrochemical cyclic voltammetry curves of as-grown NiSe₂ foam at different potential scan rates tuning from 20 mV/s to 200 mV/s with an interval point of 20 mV/s.

7. The comparison of our catalysts to other available low-cost electrocatalysts

Table S1. The comparison on the catalytic properties of our catalysts with other available non-noble HER electrocatalysts in the literatures. Here j_0 is the exchange current density, η_{10} , η_{20} and η_{100} correspond to the potentials vs RHE at current densities of 10 mA/cm², 20 mA/cm² and 100 mA/cm², respectively.

Catalyst	Tafel slope	η_{10}	η_{20}	η_{100}	j_0	Source
WS _{2(1-x)Se_{2x}} /NiSe ₂	46.7 mV/dec	88 mV	105 mV	141 mV	215 μ A/cm ²	This work
WS ₂ /NiSe ₂	54.7 mV/dec	108 mV	165 mV	115 mV	127 μ A/cm ²	This work
NiSe ₂ nanosheet	32 mV/dec	117 mV			4.7 μ A/cm ²	<i>Angew. Chem. Int. Ed.</i> 55 , 6919 (2016)
Ni ₅ P ₄ -Ni ₂ P nanosheets	79 mV/dec	120 mV	140 mV	200 mV	116 μ A/cm ²	<i>Angew. Chem. Int. Ed.</i> 54 , 8188 (2015)
MoS _x /N-CNT	40 mV/dec	110 mV	128 mV	225 mV	33.1 μ A/cm ²	<i>Nano Lett.</i> 14 , 1228 (2014)
Li-MoS ₂	62 mV/dec	118 mV	135 mV	175 mV	63 μ A/cm ²	<i>ACS Nano</i> 8 , 4940 (2014)
CoS ₂ /RGO-CNT	51 mV/dec	142 mV	153 mV	178 mV	62.6 μ A/cm ²	<i>Angew. Chem. Int. Ed.</i> 126 , 12802 (2014)
CoSe ₂ /carbon fiber	42 mV/dec	139 mV	155 mV	184 mV	6 μ A/cm ²	<i>J. Am. Chem. Soc.</i> 136 , 4897 (2014)
CoS _{1.46} Se _{0.54} NWs/CFP	45 mV/dec	104 mV	126 mV	157 mV		<i>Nano Energy</i> 18 , 1 (2015)
WS ₂ nanosheets	55 mV/dec	240 mV	280 mV		20 μ A/cm ²	<i>Nat. Mater.</i> 12 , 850 (2013)
WS ₂ nanosheets	70 mV/dec	142 mV	170 mV	288 mV	93 μ A/cm ²	<i>Energy Environ. Sci.</i> 7 , 2608 (2014)

WS _{1.56} Se _{0.44} nanoribbons	68 mV/dec	176 mV			25 $\mu\text{A}/\text{cm}^2$	<i>Adv. Funct. Mater.</i> 25 , 6077 (2015)
Ni ₂ P nanoparticles	46 mV/dec	105 mV	130 mV	180 mV	33 $\mu\text{A}/\text{cm}^2$	<i>J. Am. Chem. Soc.</i> 135 , 9267 (2013)
MoC _x nano-octahedrons	53 mV/dec	142 mV	163 mV	240 mV	23 $\mu\text{A}/\text{cm}^2$	<i>Nat. Commun.</i> 6 , 6512 (2015)
Metallic FeNiS	40 mV/dec	105 mV	140 mV	180 mV	20 $\mu\text{A}/\text{cm}^2$	<i>J. Am. Chem. Soc.</i> 137 , 11900 (2015)
Mo-W-P nanosheets/CC	52 mV/dec	100 mV		138 mV	288 $\mu\text{A}/\text{cm}^2$	<i>Energy Environ. Sci.</i> 9 , 1468 (2016)
NiP _{1.93} Se _{0.07} /carbon paper	41 mV/dec	84 mV	110 mV		100 $\mu\text{A}/\text{cm}^2$	<i>ACS Catal.</i> 5 , 6355 (2015)
CoPS/carbon paper	56 mV/dec	48 mV	65 mV		984 $\mu\text{A}/\text{cm}^2$	<i>Nat. Mater.</i> 14 , 1245 (2015)

8. Summary of the electrochemical properties among different catalysts

Table S2. Summary of the electrochemical properties of pure NiSe₂ foam, WS₂/NiSe₂ and WS_{2(1-x)}Se_{2x}/NiSe₂ hybrid electrodes. $j_{0,\text{normalized}}$ is normalized by the relative surface area.

Catalyst	η_{10}	Tafel slope	C_{dl}	$j_{0,\text{geometric}}$	Relative surface area	$j_{0,\text{normalized}}$
WS _{2(1-x)} Se _{2x} /NiSe ₂	88 mV	46.7 mV/dec	256.9 mF/cm ²	215 $\mu\text{A}/\text{cm}^2$	28.54	8.54 $\mu\text{A}/\text{cm}^2$
WS ₂ /NiSe ₂	108 mV	54.7 mV/dec	180.9 mF/cm ²	127 $\mu\text{A}/\text{cm}^2$	20.10	6.46 $\mu\text{A}/\text{cm}^2$
Pure NiSe ₂	154 mV	46.8 mV/dec	9.0 mF/cm ²	10.0 $\mu\text{A}/\text{cm}^2$	1.00	10.0 $\mu\text{A}/\text{cm}^2$